Inorganic Chemistry

Article

pubs.acs.org/IC

Synthetic-Method-Dependent Magnetic Relaxation in a Cobalt(II) Phosphonate Chain Compound

Zhong-Sheng Cai,[†] Min Ren,[†] Song-Song Bao,[†] Norihisa Hoshino,[‡] Tomoyuki Akutagawa,[‡] and Li-Min Zheng*[,†]

[†]State Key Laboratory of Coordination Chemistry, School of Chemistry and Chemical Engineering, Nanjing University, Nanjing 210093, China

[‡]Institute of Multidisciplinary Research for Advanced Materials (IMRAM), Tohoku University, Sendai 980-8577, Japan

Supporting Information

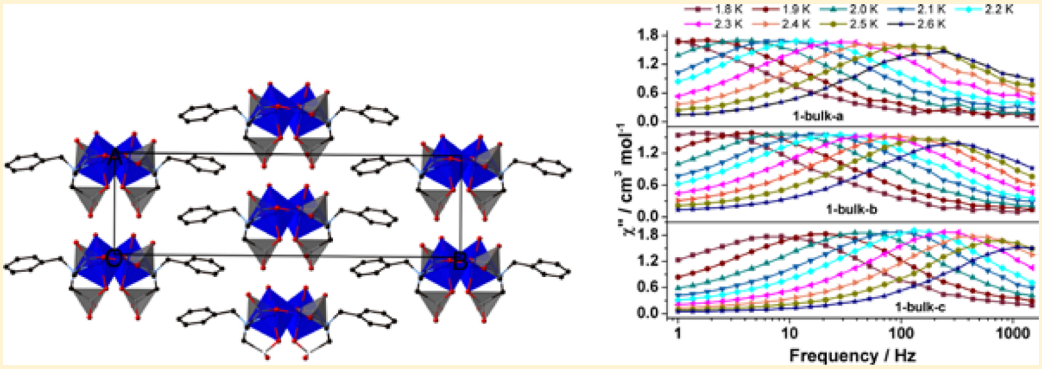

ABSTRACT: A polar cobalt(II) phosphonate $Co(bamdpH_2)(H_2O)$ (**1**) [$bamdpH_4$ = (benzylazanediyl)bis(methylene)-diphosphonic acid] is reported. It shows a linear chain structure. The neighboring chains are connected by moderately strong hydrogen bonds forming a supramolecular layer. The interlayer spaces are filled with the organic groups of the phosphonate ligands. Compound **1** displays the coexistence of single-chain magnet behavior and canted antiferromagnetism below 2.8 K. Moreover, the magnetic dynamics is strongly dependent on the synthetic methods, a phenomenon that has not been documented before.

INTRODUCTION

Owing to the potential applications in information storage and molecular spintronics there are increasing interests in the development of magnets of molecular and nanosizes.[1] As such single-molecule (SMM)[2] and single-chain magnets (SCM)[3] are highly regarded as materials for the future as they display magnetic hysteresis below their blocking temperature (T_B) and most importantly exhibit slow magnetization relaxation on fairly long time scales. In the chemistry of SCMs one chooses moment carriers with significant uniaxial anisotropy, for example, Co^{II},[4,5] Mn^{III},[6] Fe^{II},[7] Ln^{III},[8] Re^{IV},[9] and UO_2^{I}[10] to provide an Ising system with a sizable energy barrier for moment reversal. It is also important that the moments are strongly coupled within the chain (J) with negligible interchain interaction (J').[3] Thus far a number of SCMs have been reported satisfying the above conditions.[11] However, controversial examples concerning the coexistence of slow relaxation pertaining to SCM and long-range effects such as canted antiferromagnetism[12] and metamagnetism[11d,13] have also been observed. Moreover, the relaxation mechanism of SCMs is not fully understood. Although most reported SCMs show one relaxation process, dual-relaxation processes are found in a few cases.[13d,14]

To elaborate on these unusual forms of magnetism, we report a case of a new cobalt phosphonate, namely, $Co(bamdpH_2)(H_2O)$ (**1**), where $bamdpH_4$ represents (benzylazanediyl)bis(methylene)diphosphonic acid [$C_6H_5CH_2N(CH_2PO_3H_2)_2$]. This compound crystallizes in a polar space group, where considerable frequency dependence of the ac susceptibilities is observed within a canted antiferromagnetic ground state below 2.8 K. More interestingly, the relaxation property of the compound is dependent on the samples obtained under different synthetic conditions. A comparative study on the sample-dependent magnetic behavior of a closely related SCM compound $Co(p\text{-}Me\text{-}C_6H_5CH_2N(CH_2PO_3H)_2)(H_2O)$ (**2**)[5] is also presented.

EXPERIMENTAL SECTION

Materials and Measurements. The reagents and solvents employed were obtained from commercial sources and used without further purification. ((Benzylazanediyl)bis(methylene))diphosphonic acid ($bamdpH_4$) was prepared according to the literature.[15] Elemental analyses for C, H, and N were performed on an Elementar Vario

Received: September 6, 2014
Published: November 13, 2014

MICRO elemental analyzer. Infrared spectra were recorded on a Bruker TENSOR 27 IR spectrometer with pressed KBr pellets in the 400−4000 cm^{-1} region. Thermogravimetric analyses were performed on a METTLER TOLEDO TGA/DSC 1 STARe instrument in the range of 30−800 °C under nitrogen flow at a heating rate of 10 °C min^{-1}. Powder X-ray diffraction patterns were recorded on a Bruker D8 ADVANCE XRD instrument using Cu Kα radiation. Magnetic susceptibility data were obtained on polycrystalline samples using a Quantum Design MPMS-XL7 SQUID magnetometer.

Synthesis of 1-bulk-a. $Co(NO_3)_2{\cdot}6H_2O$ (58.3 mg, 0.2 mmol) and bamdpH_4 (57.9 mg, 0.2 mmol) were added to 8 mL of distilled water, and the pH value was adjusted to 3.60 with 0.5 M NaOH. Then the mixture was transferred to a 25 mL Teflon-lined autoclave and kept at 140 °C for 3 days. After cooling to room temperature, red crystals were obtained. Crystals were washed with distilled water and dried in air. Yield: 20.0 mg (27% based on Co). Anal. Calcd for $C_9H_{15}CoNO_7P_2$: C, 29.21; H, 4.09; N, 3.78. Found: C, 29.31; H, 4.37; N, 3.74. IR (KBr, cm^{-1}): 3577(s), 3337(s), 3244(m), 3023(w), 2967(w), 2896(w), 2336(w), 1649(m), 1239(m), 1204(m), 1171(s), 1135(s), 1029(s), 955(s), 915(s), 861(w), 833(w), 787(w), 744(m), 703(m), 631(m), 578(m), 559(m), 458(m), 426(w).

Synthesis of 1-bulk-b. $Co(CH_3COO)_2{\cdot}4H_2O$ (49.9 mg, 0.2 mmol) and bamdpH_4 (58.2 mg, 0.2 mmol) were added to 6 mL of distilled water, and the pH value was adjusted to 3.54 with 0.5 M HNO_3. Then the mixture was transferred to a 25 mL Teflon-lined autoclave and kept at 140 °C for 3 days. After cooling to room temperature, red crystals were obtained, washed with distilled water, and dried in air. Yield: 23.2 mg (31% based on Co). Anal. Calcd for $C_9H_{15}CoNO_7P_2$: C, 29.21; H, 4.09; N, 3.78. Found: C, 29.21; H, 4.17; N, 3.86.

Synthesis of 1-bulk-c. $Co(CH_3COO)_2{\cdot}4H_2O$ (49.1 mg, 0.2 mmol) and bamdpH_4 (94.7 mg, 0.32 mmol) were added to 6 mL of distilled water, and the pH value was about 3.48 without adding any other reagent. Then the mixture was transferred to a 25 mL Teflon-lined autoclave and kept at 140 °C for 3 days. After cooling to room temperature, red crystals were obtained, washed with distilled water, and dried in air. Yield: 24.5 mg (33% based on Co). Anal. Calcd for $C_9H_{15}CoNO_7P_2$: C, 29.21; H, 4.09; N, 3.78. Found: C, 29.36; H, 4.50; N, 3.77.

Synthesis of 1-bulk-d. $Co(NO_3)_2{\cdot}6H_2O$ (60.9 mg, 0.2 mmol) and bamdpH_4 (58.4 mg, 0.2 mmol) were added to 6 mL of distilled water, and the pH value was adjusted to 3.49 using 33.7 mg of 4,4′-bipyridine. Then the mixture was transferred to a 25 mL Teflon-lined autoclave and kept at 140 °C for 3 days. After cooling to room temperature, red crystals were obtained, washed with distilled water, and dried in air. Yield: 20.0 mg (27% based on Co).

Synthesis of 1-bulk-e. $Co(NO_3)_2{\cdot}6H_2O$ (60.7 mg, 0.2 mmol) and bamdpH_4 (59.5 mg, 0.2 mmol) were added to 6 mL of distilled water, and the pH value was adjusted to 3.15 using 27.1 mg of 4,4′-bipyridine. Then the mixture was transferred to a 25 mL Teflon-lined autoclave and kept at 140 °C for 3 days. After cooling to room temperature, red crystals were obtained, washed with distilled water, and dried in air. Yield: 11.8 mg (16% based on Co).

X-ray Crystallographic Analyses. Single crystals were selected for indexing and intensity data collection on a Bruker SMART APEX CCD diffractometer using graphite-monochromatized Mo Kα radiation (λ = 0.71073 Å) at room temperature. Data were integrated using the Siemens SAINT program[16] with the intensities corrected for Lorentz factor, polarization, air absorption, and absorption due to variation in the path length through the detector face plate. Absorption corrections were applied. Structures were solved by direct methods and refined on F^2 by full-matrix least-squares using SHELXTL.[17] All non-hydrogen atoms were located from the Fourier maps and refined anisotropically. All H atoms were refined isotropically with the isotropic vibration parameters related to the non-hydrogen atoms to which they are bonded. Crystallographic data of compound **1** are listed in Table 1, and selected bond lengths and angles are given in Table 2.

Table 1. Crystallographic Data for 1

empirical formula	$C_9H_{15}CoNO_7P_2$
fw	370.09
cryst syst	monoclinic
space group	*Cc*
a (Å)	8.5361(3)
b (Å)	26.5298(11)
c (Å)	6.2175(2)
β (deg)	113.3120(10)
V (Å^3), *Z*	1293.08(56), 4
D_c (g cm^{-3})	1.901
F (000)	756
*R*1,[a] *wR*2[b] [$I > 2\sigma(I)$]	0.0191, 0.0428
*R*1,[a] *wR*2[b] (all data)	0.0202, 0.0431
goodness-of-fit	0.997
Flack parameter	0.02(1)
$(\Delta\rho)_{max}$, $(\Delta\rho)_{min}$ (e Å^{-3})	0.339, −0.335
CCDC number	905563

[a] $R_1 = \Sigma||F_o| - |F_c||/\Sigma|F_o|$. [b] $wR_2 = [\Sigma w(F_o^2 - F_c^2)^2/\Sigma w(F_o^2)^2]^{1/2}$.

Table 2. Selected Bond Lengths (Angstroms) and Angles (degrees) for 1[a]

Co1−O5B	2.044(2)	Co1−O4A	2.122(2)
Co1−O1W	2.111(2)	Co1−O4	2.161(2)
Co1−O1	2.120(2)	Co1−N1	2.257(2)
O5B−Co1−O1W	91.5(1)	O5B−Co1−O4	165.0(1)
O5B−Co1−O1	93.8(1)	O1W−Co1−O4	82.9(1)
O1W−Co1−O1	174.5(1)	O1−Co1−O4	91.7(1)
O5B−Co1−O4A	84.7(1)	O4A−Co1-O4	108.8(1)
O1W−Co1−O4A	88.4(1)	O5B−Co1−N1	82.8(1)
O1−Co1−O4A	92.7(1)	O1W−Co1−N1	100.0(1)
O1−Co1−N1	80.0(1)	P2−O4−Co1C	116.3(1)
O4A−Co1−N1	165.1(1)	P2−O4−Co1	114.0(1)
O4−Co1−N1	84.4(1)	P2−O5−Co1D	152.4(1)
P1−O1−Co1	114.0(1)	C3−N1−Co1	109.4(1)
C1−N1−Co1	105.8(1)	Co1A−O4A−Co1	122.2(1)
C2−N1−Co1	107.6(1)		

[a] Symmetry codes: (A) *x*, −*y* + 1, *z* + 0.5; (B) *x*, *y*, *z* + 1; (C) *x*, −*y* + 1, *z* − 0.5; (D) *x*, *y*, *z* − 1.

RESULTS AND DISCUSSION

Crystal Structure of 1. Although samples **1-bulk-a**−**e** were synthesized under different experimental conditions using different starting materials and/or pH adjusters, general characterization such as powder XRD, IR, TG, and elemental analyses reveals that they are identical in both composition and structure (Figures S1−S3, Supporting Information). Thus, a single crystal was picked up from **1-bulk-a**. Single-crystal structural analysis reveals that **1** crystallizes in a polar space group *Cc*. The asymmetric unit consists of one Co^{II}, one bamdpH_2^{2-}, and one coordinated water molecule. The Co1 atom has a distorted octahedral environment surrounded by one nitrogen atom, four phosphonate oxygen atoms, and one water molecule [Co1−O 2.044(2)−2.161(2) Å, Co1−N 2.257(2) Å] (Figure 1a). The equivalent Co1 atoms are bridged by μ_3-O(P) and O−P−O units forming a zigzag chain running along the *c* axis (Figure 1b). The Co···Co distance over the μ_3-O(P) is 3.750(1) Å. Strong hydrogen-bond interactions are found between the chains [O6···O2^i 2.544(2) Å; O6−H6A−O2^i 172.1(1)°; symmetry code (i) *x* + 1, *y*, *z*], resulting in a supramolecular layer in the *ac* plane (Figure S4, Supporting

dx.doi.org/10.1021/ic5021737 | Inorg. Chem. 2014, 53, 12546−12552

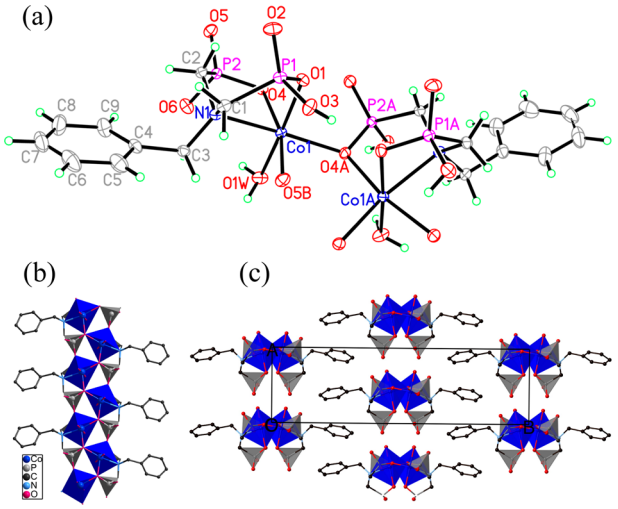

Figure 1. (a) Building unit of compound **1** with atom-labeling scheme (40% probability). (b) Chain structure of **1**. (c) Structure of **1** packed along the *c* axis. All H atoms are omitted for clarity. CoO_5N and PO_3C polyhedra are shown in blue and gray, respectively.

Information). The layer is polar due to the alternative parallel arrangement of the positively charged $\{CoO_5N\}$ and negatively charged $\{PO_3C\}$ polyhedra along the *a* axis. The shortest Co···Co distance between the chains within the layer is 8.120(1) Å. The phenylmethyl groups reside on opposite sides of the layer. The layers are stacked along the *b* axis, resulting in a polar three-dimensional supramolecular structure (Figure 1c). The $\pi-\pi$ interactions are negligible between the neighboring phenyl rings as the dihedral angle is 23.9(1)° and center-to-center distance is 4.208(1) Å. The shortest Co···Co distance between the layers is 11.920(1) Å.

Magnetic Properties. The magnetic behaviors of samples **1-bulk-a**–**c** are studied in detail. Figure 2a shows the dc magnetic susceptibilities (H = 2 kOe) plotted as $\chi_M T$ vs T which are almost the same for the three samples. $\chi_M T$ at 300 K is 3.14/3.11/3.13 cm^3 K mol^{-1} per Co for **1-bulk-a**/**1-bulk-b**/**1-bulk-c**, much larger than the spin-only value of 1.88 cm^3 K mol^{-1} expected for spin S = 3/2 with g = 2.0 due to the orbital contribution from the octahedral Co^{II} ion. The susceptibility data above 100 K follow the Curie–Weiss law with the Curie constant (C) and Weiss constant (θ) of 3.43/3.18/3.44 cm^3 K mol^{-1} and −23.7/−28.5/−27.6 K for **1-bulk-a**/**1-bulk-b**/**1-bulk-c**, respectively (Figure S5, Supporting Information). The Weiss temperature θ, slightly more negative than that expected for the presence of spin–orbit coupling, indicates antiferromagnetic (AF) interaction between nearest neighbors.[18] Upon cooling, $\chi_M T$ decreases continuously and approaches a minimum of 0.68/0.72/0.73 cm^3 K mol^{-1} at 8 K followed by a sharp increase to a value of 1.67/1.90/1.85 cm^3 K mol^{-1} at 3.5 K, below which $\chi_M T$ decreases again. Since the chain could be considered as an isotropic Heisenberg chain with S = 3/2 in the high-temperature region, Fisher's chain model[19] scaled to S = 3/2 is applied to simulate the susceptibility data above 100 K (Figure S6, Supporting Information). The best fits result in intrachain coupling constants J = −8.99/−10.07/−9.94 K and g = 2.71/2.70/2.70 for **1-bulk-a**/**1-bulk-b**/**1-bulk-c**, respectively. The g values are close to those obtained from Curie constants (g = 2.71/2.60/2.71).

The zero-field-cooled (ZFC) and field-cooled (FC, H_{dc} = 0.8 or 10 Oe) magnetic susceptibilities for **1-bulk-a** show a

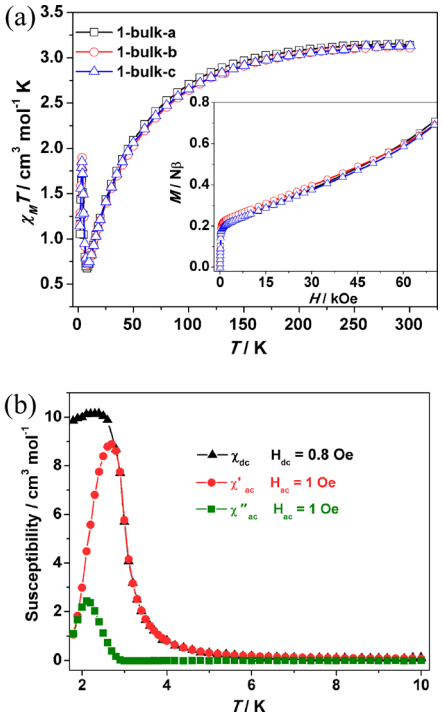

Figure 2. (a) $\chi_M T$ vs T plots of the three samples. (Inset) M vs H plots. (b) Temperature dependence of the dc and ac susceptibilities for sample **1-bulk-a**. Solid lines are a guide for the eye.

bifurcation below 2.8 K, indicating the onset of a blocking of the moments (Figures 2b and S7, Supporting Information). The sharpness of the blocking and its independence on the applied field suggests the occurrence of long-range magnetic ordering (LRO). The isothermal magnetization displays no hysteresis loop down to 1.8 K (Figure S8, Supporting Information). The initial magnetization is almost linear in field until it saturates at ca. 0.2 $N\beta$ and then increases gradually to 0.70 ± 0.01 $N\beta$ at 70 kOe (Figure 2a, inset). The latter values are much lower than that for a fully aligned moment of 2.3 $N\beta$. The behavior can be regarded as a canted antiferromagnet with a canting angle estimated from $\sin^{-1}(0.2/2.3)$ of 5°. **1-bulk-a**, **1-bulk-b**, and **1-bulk-c** behave in a similar manner.

A remarkable difference is observed in the ac susceptibility data. Figure 3 and Figures S9 and S10, Supporting Information, give the temperature-dependent ac susceptibility measured at

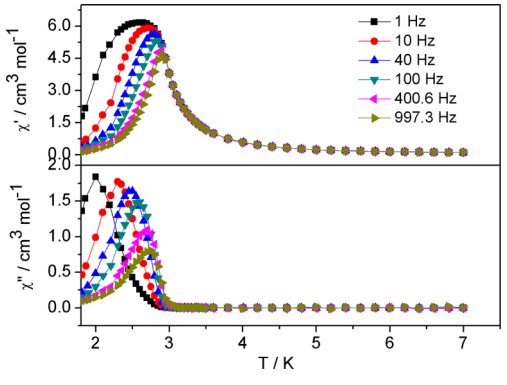

Figure 3. χ' and χ'' versus T plots with eye-guided lines of **1-bulk-a** measured at zero dc field (H_{ac} = 1.4 Oe).

dx.doi.org/10.1021/ic5021737 | Inorg. Chem. 2014, 53, 12546–12552

zero dc field (H_{ac} = 1.4 Oe) and at frequencies of 1−1500 Hz. In all cases, both the in-phase (χ') and the out-of-phase (χ'') signals show frequency dependence below 2.8 K, indicating a slow relaxation of magnetization. If we compare the χ'' signals at 1 Hz, however, it is clear that the peak appearing at 2.0 K in **1-bulk-a** vanishes in **1-bulk-b** and **1-bulk-c** (Figure S11, Supporting Information), suggesting that the relaxation in **1-bulk-a** is much slower. A least-squares fit using the Arrhénius relation $\tau(T) = \tau_0 \exp(\Delta_{eff}/k_BT)$ based on peaks in the χ'' vs T plots results in energy barriers (Δ_{eff}/k_B) and pre-exponential factors (τ_0) of 37.0/27.9/30.4 K and 1.52×10^{-9}/1.38×10^{-8}/9.22×10^{-10} s, respectively, for the three samples. The τ_0 values fall in the range found for SCMs. The parameter $f = (\Delta T_p/T_p)/\Delta \log f$ is estimated as 0.10/0.14/0.16 for **1-bulk-a**/**1-bulk-b**/**1-bulk-c**, precluding the spin-glass behaviors.[20]

The sharp blocking of the moments at 2.8 K associated with the onset of the imaginary ac susceptibility for all frequencies studied indicates a long-range magnetic ordering (LRO) in favor of SCM behavior. Oka et al. has recently shown that LRO can be established for a diamond chain isolated at 17 Å without any chemical connection between the chains.[21] They argue for the first time that the magnetic domain structure within the chains of such a network will dominate the dynamics.[21] Consequently, the dynamics are similar to that for SCMs, as the extracted parameters above demonstrate, due to the very anisotropic domain shape. The results are consistent with those found for the mineral $K_2Co^{II}_3(OH)_2(SO_4)_3(H_2O)_2$, where a strong frequency dependence of the ac susceptibilities was found within the LRO state determined by neutron diffraction,[22] which was associated with elongated domain.

The difference in dynamics could be clearly visualized in the χ', χ'' vs frequency curves, measured between 1.8 and 2.6 K under zero dc field (H_{ac} = 1.4 Oe). χ'' increases at the expense of χ' (Figures S12, Supporting Information, and 4a). The peaks of χ'' signals at the same temperature shift to higher frequencies from **1-bulk-a** to **1-bulk-c**, revealing the gradual decrease of relaxation time. The relaxation time can be extracted by fitting the Cole−Cole plots[23] using the generalized Debye model. A least-squares fit based on the Arrhenius relationship results in parameters Δ_{eff}/k_B = 34.1/30.3/29.8 K and $\tau_0 = 1.78 \times 10^{-9}$/ 4.83×10^{-9}/1.42×10^{-9} s for **1-bulk-a**, **1-bulk-b**, and **1-bulk-c**, respectively (Figure 4b). The parameters are slightly different from those obtained from the temperature-dependent ac susceptibility data. However, the frequency dependence fit could be more reliable because the whole curve is used for fitting instead of peak maximum only. The distribution coefficient α values are in the range of 0.29−0.41/0.28−0.40/0.23−0.36 for the three samples with decreasing temperature (Figure S13, Tables S1−S3, Supporting Information), indicating a relatively broad distribution of the relaxation time. The large distribution of the relaxation time is also demonstrated by the fact that χ'' shows signals below 2.8 K, where the ZFC-FC curves also show bifurcation.

Observation of different magnetic dynamics in samples **1-bulk-a**, **1-bulk-b**, and **1-bulk-c** is unprecedented because they are structurally and chemically the same. Considering that compound **1** crystallizes in a polar space group *Cc*, we wonder whether the direction of the polar axis could have any impact on the magnetic behavior. Thus, five single crystals were each randomly selected from **1-bulk-a** and **1-bulk-b**, respectively, and subjected to structural determination. The results demonstrate that all show the same structure with almost the same cell parameters (Table S4, Supporting Information). The

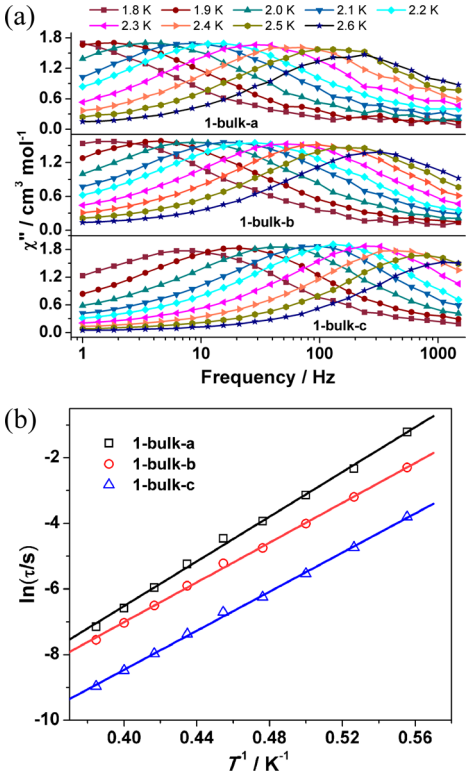

Figure 4. (a) χ'' vs frequency, and (b) $\ln(\tau/s)$ vs T^{-1} plots for samples **1-bulk-a**, **1-bulk-b**, and **1-bulk-c**. Solid lines are a guide for the eye in a and best fitting in b.

only difference is the Flack parameter. For **1-bulk-a**, the Flack parameter is close to zero for one crystal, while it is 0.49−0.76 for the other four crystals. For **1-bulk-b**, the Flack parameter is close to zero for three crystals but 0.79−0.80 for the other two crystals. If structures with Flack parameters of 0 and 1 can be viewed as a pair of polar isomers, both **1-bulk-a** and **1-bulk-b** contain a mixture of two isomers. Therefore, observation of a single relaxation process in each sample cannot be explained by the presence of two polar isomers.

It is noted that samples **1-bulk-a**, **1-bulk-b**, and **1-bulk-c** were synthesized under similar experimental conditions except for the inorganic salts. The NO_3^- anion is used in preparing sample **1-bulk-a**, while CH_3COO^- is employed in preparing sample **1-bulk-c**. For **1-bulk-b**, both NO_3^- and CH_3COO^- are involved in the reaction mixture. As demonstrated by Sessoli and co-workers, the crystalline defects and chemical modifications can also be present in the undoped pure compound on the order of a few per thousand spins.[11a,24,25] Although the anions are not involved in the structures of the final products, they could disturb the crystallization process of compound **1**, generating different amounts of defects within the crystalline samples. Unfortunately, direct observation or analysis of the absolute amounts of the defects is difficult, especially for molecular systems.[25] However, defects do play a key role in the magnetization relaxation of SCMs by dividing the chains into short segments.[11a,24]

It is well known that excitations nucleating close to a defect site cost one-half the energy of those inside the chain in the SCMs. At high temperature, the magnetic correlation length (ξ) is shorter than the chain length ($\langle L \rangle$) and the spin flip occurs with $\Delta = 4J$. At low temperature, ξ is much longer than $\langle L \rangle$; hence, $\Delta = 2J$. The crossover temperature from the

dx.doi.org/10.1021/ic5021737 | Inorg. Chem. 2014, 53, 12546−12552

infinite-size to finite-size regime depends on J and $\langle L \rangle$ and becomes higher for shorter chains. As expected from the Glauber model in a 1D anisotropic system, a linear fit in the $\ln(\chi' T)$ vs T^{-1} plot in the temperature range 2.9−3.5 K gives Δ_ξ = 19.9/20.2/22.2 K for **1-bulk-a**/**1-bulk-b**/**1-bulk-c**, respectively, on the basis of the expression $\chi T = C_{\text{eff}} \exp(\Delta_\xi / k_B T)$, where C_{eff} is the effective Curie constant and Δ_ξ is the energy required to create a domain wall along the chain (Figure S14, Supporting Information). Therefore, the exchange coupling constant within the chain can be estimated as $|J|$ = 10.0/10.1/11.1 K for the three samples, which are close to those obtained from Fisher's chain model (J = −8.99/−10.07/−9.94 K). The energy barriers are expected to be ca. 40 and 20 K in the infinite-size and finite-size regions, respectively. The energy barriers of the three samples obtained based on the Arrhenius law (29.8−34.1 K) are between them, indicating the coexistence of chains in the two regimes.

The effective chain lengths could be related to the defects in the three samples. As demonstrated by Bogani et al.,[24] the higher concentration of defects will contribute to higher crossover temperature, i.e., higher deviation temperature from the linear dependence of $\ln(\chi' T)$ vs T^{-1} curve. The deviation temperatures are 2.86/2.89/2.93 K for **1-bulk-a**/**1-bulk-b**/**1-bulk-c** (Figure S14, Supporting Information), suggesting the increase of defects in the sequence of **1-bulk-a** < **1-bulk-b** < **1-bulk-c**. In addition, Figure 4b shows that the relaxation time decreases in the sequence **1-bulk-a** > **1-bulk-b** > **1-bulk-c**, indicating that the effective chain length decreases in the same sequence.[24a] Thus, a higher concentration of defects contributes to a shorter effective chain length in the three samples.

To check the effect of the other templates such as organic molecules, samples **1-bulk-d** and **1-bulk-e** were obtained following a similar synthetic procedure to sample **1-bulk-a** except that the pH was adjusted by 4,4′-bipyridine to 3.49 and 3.15, respectively. The SCM behavior is again observed for **1-bulk-d** and **1-bulk-e** with energy barriers of 39.6/40.5 K and τ_0 values of 1.30 × 10^{-10}/2.67 × 10^{-10} s, respectively (Figures S15−S17, Supporting Information). The barriers are close to that expected for the SCM in the infinite region. The results suggest that the length of chain segments in compound **1** may be adjusted by the presence of suitable counteranions or organic templates. The experiments are reproducible, although the values of Δ_{eff} and τ_0 can be slightly different.

With the above observations, we wonder whether it is possible to observe two relaxation processes in a SCM system simply by changing the synthetic condition. Hence, we examine in a similar eye the properties of the structurally similar compound Co(*p*-Me-$C_6H_5CH_2N(CH_2PO_3H)_2)(H_2O)$ (**2**) in which the phosphonate ligand has an additional methyl group.[5] This compound crystallizes in a centrosymmetric ($P2_1/c$) instead of a polar space group and has been described to be a SCM.[5] For a comparison, three samples of **2** were hydrothermally synthesized at 140 °C using different cobalt salts and pH adjusters, e.g., $Co(NO_3)_2$/*p*-Me-$C_6H_5CH_2N(CH_2PO_3H_2)_2$/NaOH for **2-bulk-a**, $Co(CH_3COO)_2$/*p*-Me-$C_6H_5CH_2N(CH_2PO_3H_2)_2$/$HNO_3$ for **2-bulk-b**, and $Co(CH_3COO)_2$/*p*-Me-$C_6H_5CH_2N(CH_2PO_3H_2)_2$ for **2-bulk-c**. Although the synthetic conditions are different from that reported in the literature where tetramethylammonium chloride was involved and the reaction was carried out at 180 °C for 4 days,[5b] samples **2-bulk-a**, **2-bulk-b**, and **2-bulk-c** are the same as compound **2**, as proved by powder XRD and IR measurements (Figures S18 and S19, Supporting Information).

The frequency-dependent ac susceptibility data of the three samples are measured at 1.8−2.2 K (Figures S20, Supporting Information, and 5a). Slow magnetization relaxation is observed

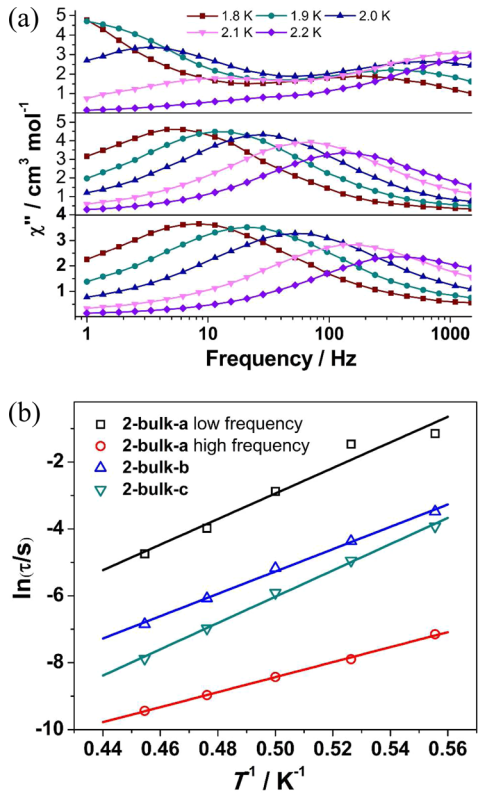

Figure 5. (a) χ'' vs frequency plots. (b)Logarithmic magnetization relaxation time (τ) versus T^{-1} plots with Arrhenius fitting for samples **2-bulk-a**, **2-bulk-b**, and **2-bulk-c**.

in all cases as expected. For samples **2-bulk-b**/**2-bulk-c**, only one relaxation process appears with energy barriers of 33.4/39.3 K and pre-exponential factors of 2.87 × 10^{-10}/7.01 × 10^{-12} s. Interestingly, **2-bulk-a** shows a double-relaxation process with energy barriers of 38.2 and 22.4 K and τ_0 of 2.66 × 10^{-10} and 2.93 × 10^{-9} s, respectively (Figures S21, Supporting Information, and 5b). Noting that the energy barrier of the high-frequency relaxation is almost one-half of that of low-frequency relaxation in sample **2-bulk-a**,[13d,14] we propose that the presence of two relaxation processes could be attributed to the coexistence of both the infinite- and the finite-size regimes in this sample.

CONCLUSIONS

We prepared five samples of a chain compound Co(bamdpH_2)-(H_2O) (**1**) under slightly different synthetic conditions using different cobalt salts or organic templates. Magnetic studies reveal that in all cases the sharp imaginary ac susceptibility can be observed at one fixed temperature for all frequencies, suggesting the occurrence of LRO. In addition, dynamics are present and similar to SCMs due to similar domain shapes. The magnetization relaxation is significantly affected by the synthetic methods and templates used, which has not been documented before in the literature. Further, observation of double-relaxation processes in sample **2-bulk-a** suggests that the origin of the dual relaxation in SCM systems could be due to the presence of both the infinite- and the finite-size regimes.

dx.doi.org/10.1021/ic5021737 | *Inorg. Chem.* 2014, 53, 12546−12552

This work highlights the importance of defects in the understanding of magnetic dynamics of structures having chains of magnetic moment carriers and also provides a new route to control the chain length and hence the energy barrier of SCMs.

■ ASSOCIATED CONTENT

Supporting Information

Structural data, IR, PXRD, TG, and additional magnetic data. This material is available free of charge via the Internet at http://pubs.acs.org.

■ AUTHOR INFORMATION

Corresponding Author

*E-mail: lmzheng@nju.edu.cn.

Notes

The authors declare no competing financial interest.

■ ACKNOWLEDGMENTS

Financial support by the National Basic Research Program of China (2010CB923402, 2013CB922102), the NSF of Jiangsu Province of China (No. BK2009009), and the NSF of China (No. 21371094) is acknowledged. We appreciate Prof. M. Kurmoo for kind proof-reading and comments and Prof. E. Coronado for valuable discussions. We also thank Prof. Li Pi for kind help in magnetic measurements.

■ REFERENCES

(1) (a) Bogani, L.; Wernsdorfer, W. *Nat. Mater.* **2008**, *7*, 179−186. (b) Ardavan, A.; Blundell, S. J. *J. Mater. Chem.* **2009**, *19*, 1754−1760. (c) Camarero, J.; Coronado, E. *J. Mater. Chem.* **2009**, *19*, 1678−1684.

(2) (a) Caneschi, A.; Gatteschi, D.; Sessoli, R.; Barra, A. L.; Brunel, L. C.; Guillot, M. *J. Am. Chem. Soc.* **1991**, *113*, 5873−5874. (b) Gatteschi, D.; Sessoli, R.; Villain, J. *Molecular Nanomagnets*; Oxford University Press: Oxford, U.K., 2006.

(3) (a) Glauber, R. J. *J. Math. Phys.* **1963**, *4*, 294−307. (b) Caneschi, A.; Gatteschi, D.; Lalioti, N.; Sangregorio, C.; Sessoli, R.; Venturi, G.; Vindigni, A.; Rettori, A.; Pini, M. G.; Novak, M. A. *Angew. Chem., Int. Ed.* **2001**, *40*, 1760−1763. (c) Coulon, C.; Miyasaka, H.; Clérac, R. *Struct. Bonding (Berlin)* **2006**, *122*, 163−206.

(4) (a) Liu, T. F.; Fu, D.; Gao, S.; Zhang, Y.-Z.; Sun, H.-L.; Su, G.; Liu, Y. J. *J. Am. Chem. Soc.* **2003**, *125*, 13976−13977. (b) Lescouëzec, R.; Vaissermann, J.; Ruiz-Pérez, C.; Llorest, F.; Carrasco, R.; Julve, M.; Verdaguer, M.; Dromzee, Y.; Gatteschi, D.; Wernsdorfer, W. *Angew. Chem., Int. Ed.* **2003**, *42*, 1483−1486. (c) Zheng, Y.-Z.; Tong, M.-L.; Zhang, W.-X.; Chen, X.-M. *Angew. Chem., Int. Ed.* **2006**, *45*, 6310−6314. (d) Zhang, X.-M.; Hao, Z.-M.; Zhang, W.-X.; Chen, X.-M. *Angew. Chem., Int. Ed.* **2007**, *46*, 3456−3459. (e) Coronado, E.; Galán-Mascarós, J. R.; Martí-Gastaldo, C. *J. Am. Chem. Soc.* **2008**, *130*, 14987−14989. (f) Liu, T.; Zhang, Y.-J.; Kanegawa, S.; Sato, O. *J. Am. Chem. Soc.* **2010**, *132*, 8250−8251. (g) Dong, D.-P.; Liu, T.; Kanegawa, S.; Kang, S.; Sato, O.; He, C.; Duan, C.-Y. *Angew. Chem., Int. Ed.* **2012**, *51*, 5119−5123. (h) Hoshino, N.; Iijima, F.; Newton, G. N.; Yoshida, N.; Shiga, T.; Nojiri, H.; Nakao, A.; Kumai, R.; Murakami, Y.; Oshio, H. *Nat. Chem.* **2012**, *4*, 921−926. (i) Tangoulis, V.; Lalia-Kantouri, M.; Gdaniec, M.; Papadopoulos, Ch.; Miletic, V.; Czapik, A. *Inorg. Chem.* **2013**, *52*, 6559−6569. (j) Vaz, M. G. F.; Cassaro, R. A. A.; Akpinar, H.; Schlueter, J. A.; Lahti, P. M.; Novak, M. A. *Chem.—Eur. J.* **2014**, *20*, 5460−5467. (k) Ma, X.; Zhang, Z.; Shi, W.; Li, L.; Zou, J.; Cheng, P. *Chem. Commun.* **2014**, *50*, 6340−6342.

(5) (a) Sun, Z.-M.; Prosvirin, A. V.; Zhao, H.-H.; Mao, J.-G.; Dunbar, K. R. *J. Appl. Phys.* **2005**, *97*, 10B305/1−10B305/3. (b) Palii, A. V.; Reu, O. S.; Ostrovsky, S. M.; Klokishner, S. I.; Tsukerblat, B. S.; Sun, Z.-M.; Mao, J.-G.; Prosvirin, A. V.; Zhao, H.-H.; Dunbar, K. R. *J. Am. Chem. Soc.* **2008**, *130*, 14729−14738.

(6) (a) Clérac, R.; Miyasaka, H.; Yamashita, M.; Coulon, C. *J. Am. Chem. Soc.* **2002**, *124*, 12837−12844. (b) Bai, Y.-L.; Tao, J.; Wernsdorfer, W.; Sato, O.; Huang, R.-B.; Zheng, L.-S. *J. Am. Chem. Soc.* **2006**, *128*, 16428−16429. (c) Xu, H.-B.; Wang, B.-W.; Pan, F.; Wang, Z.-M.; Gao, S. *Angew. Chem., Int. Ed.* **2007**, *46*, 7388−7392. (d) Bernot, K.; Luzon, J.; Sessoli, R.; Vindigni, A.; Thion, J.; Richeter, S.; Leclercq, D.; Larionova, J.; van der Lee, A. *J. Am. Chem. Soc.* **2008**, *130*, 1619−1627. (e) Wang, T.-T.; Ren, M.; Bao, S.-S.; Liu, B.; Pi, L.; Cai, Z.-S.; Zheng, Z.-H.; Xu, Z.-L.; Zheng, L.-M. *Inorg. Chem.* **2014**, *53*, 3117−3125. (f) Chen, X.; Wu, S.-Q.; Cui, A.-L.; Kou, H.-Z. *Chem. Commun.* **2014**, *50*, 2120−2122.

(7) (a) Wang, S.; Zuo, J.-L.; Gao, S.; Song, Y.; Zhou, H.-C.; Zhou, Y.-Z.; You, X.-Z. *J. Am. Chem. Soc.* **2004**, *126*, 8900−8901. (b) Kajiwara, T.; Nakano, M.; Kaneko, Y.; Takaishi, S.; Ito, T.; Yamashita, M.; Igashira-Kamiyama, A.; Nojiri, H.; Ono, Y.; Kojima, N. *J. Am. Chem. Soc.* **2005**, *127*, 10150−10151. (c) Venkatakrishnan, T. S.; Sahoo, S.; Bréfuel, N.; Duhayon, C.; Paulsen, C.; Barra, A.-L.; Ramasesha, S.; Sutter, J.-P. *J. Am. Chem. Soc.* **2010**, *132*, 6047−6056. (d) Liu, T.; Zheng, H.; Kang, S.; Shiota, Y.; Hayami, S.; Mito, M.; Sato, O.; Yoshizawa, K.; Kanegawa, S.; Duan, C.-Y. *Nat. Commun.* **2013**, *4*, 2826−2832.

(8) (a) Bogani, L.; Sangregorio, C.; Sessoli, R.; Gatteschi, D. *Angew. Chem., Int. Ed.* **2005**, *44*, 5817−5821. (b) Bernot, K.; Bogani, L.; Caneschi, A.; Gatteschi, D.; Sessoli, R. *J. Am. Chem. Soc.* **2006**, *128*, 7947−7956.

(9) (a) Harris, T. D.; Bennett, M. V.; Clérac, R.; Long, J. R. *J. Am. Chem. Soc.* **2010**, *132*, 3980−3988. (b) Feng, X.; Liu, J.; Harris, T. D.; Hill, S.; Long, J. R. *J. Am. Chem. Soc.* **2012**, *134*, 7521−7529.

(10) Mougel, V.; Chatelain, L.; Hermle, J.; Caciuffo, R.; Colineau, E.; Tuna, F.; Magnani, N.; de Geyer, A.; Pécaut, J.; Mazzanti, M. *Angew. Chem., Int. Ed.* **2014**, *53*, 819−823.

(11) (a) Bogani, L.; Vindigni, A.; Sessoli, R.; Gatteschi, D. *J. Mater. Chem.* **2008**, *18*, 4750−4758. (b) Miyasaka, H.; Julve, M.; Yamashita, M.; Clérac, R. *Inorg. Chem.* **2009**, *48*, 3420−3437. (c) Sun, H.-L.; Wang, Z.-M.; Gao, S. *Coord. Chem. Rev.* **2010**, *254*, 1081−1100. (d) Zhang, W.-X.; Ishikawa, R.; Breedlove, B.; Yamashita, M. *RSC Adv.* **2013**, *3*, 3772−3798.

(12) Bhowmick, I.; Hillard, E. A.; Dechambenoit, P.; Coulon, C.; Harris, T. D.; Clérac, R. *Chem. Commun.* **2012**, *48*, 9717−9719.

(13) (a) Coulon, C.; Clérac, R.; Wernsdorfer, W.; Colin, T.; Miyasaka, H. *Phys. Rev. Lett.* **2009**, *102*, 167204/1−167204/4. (b) Miyasaka, H.; Takayama, K.; Saitoh, A.; Furukawa, S.; Yamashita, M.; Clérac, R. *Chem.—Eur. J.* **2010**, *16*, 3656−3662. (c) Boeckmann, J.; Wriedt, M.; Näther, C. *Chem.—Eur. J.* **2012**, *18*, 5284−5289. (d) Toma, L. M.; Ruiz-Pérez, C.; Pasán, J.; Wernsdorfer, W.; Lloret, F.; Julve, M. *J. Am. Chem. Soc.* **2012**, *134*, 15265−15268. (e) Zhang, W.-X.; Shiga, T.; Miyasaka, H.; Yamashita, M. *J. Am. Chem. Soc.* **2012**, *134*, 6908−6911.

(14) (a) Toma, L. M.; Ruiz-Pérez, C.; Lloret, F.; Julve, M. *Inorg. Chem.* **2012**, *51*, 1216−1218. (b) Ferrando-Soria, J.; Pardo, E.; Ruiz-García, R.; Cano, J.; Lloret, F.; Julve, M.; Journaux, Y.; Pasán, J.; Ruiz-Pérez, C. *Chem.—Eur. J.* **2011**, *17*, 2176−2188.

(15) Sun, Z.-M.; Yang, B.-P.; Sun, Y.-Q.; Mao, J.-G.; Clearfield, A. *J. Solid. State. Chem.* **2003**, *176*, 62−68.

(16) *SAINT, Program for Data Extraction and Reduction*; Siemens Analytical X-ray Instruments: Madison, WI, 1994−1996.

(17) *SHELXTL (version 5.0), Reference Manual*; Siemens Industrial Automation, Analytical Instruments: Madison, WI, 1995.

(18) Kurmoo, M. *Chem. Soc. Rev.* **2009**, *38*, 1353−1379.

(19) (a) Fisher, M. E. *Am. J. Phys.* **1964**, *32*, 343−346. (b) Kahn, O. *Molecular Magnetism*; VCH Publisher, Inc.: Weinheim, 1993.

(20) Mydosh, J. A. *Spin Glasses: an Experimental Introduction*; Taylor & Francis: London, Washington, DC, 1993; p 67.

(21) Oka, Y.; Inoue, K.; Kumagai, H.; Kurmoo, M. *Inorg. Chem.* **2013**, *52*, 2142−2149.

(22) Vilminot, S.; Baker, P. J.; Blundell, S.; Sugano, T.; Andre, G.; Kurmoo, M. *Chem. Mater.* **2010**, *22*, 4090−4095.

(23) Cole, K. S.; Cole, R. H. *J. Chem. Phys.* **1941**, *9*, 341−351.

(24) (a) Pini, M. G.; Rettori, A.; Bogani, L.; Lascialfari, A.; Mariani, M.; Caneschi, A.; Sessoli, R. *Phys. Rev. B* **2011**, *84*, 094444/1−094444/15. (b) Bogani, L.; Sessoli, R.; Pini, M. G.; Rettori, A.; Novak, M. A.; Rosa, P.; Massi, M.; Fedi, M. E.; Giuntini, L.; Caneschi, A.; Gatteschi, D. *Phys. Rev. B* **2005**, *72*, 064406/1−064406/10.
(25) Bogani, L.; Caneschi, A.; Fedi, M.; Gatteschi, D.; Massi, M.; Novak, M. A.; Pini, M. G.; Rettori, A.; Sessoli, R.; Vindigni, A. *Phys. Rev. Lett.* **2004**, *92*, 207204/1−207204/4.